Cell Reports, Volume *45*

Supplemental information

Ski2-like helicase ASCC3 unwinds DNA upon fork stalling to control replication stress responses

Shixin Cui, Nicole L. Batenburg, Yan Coulombe, Aruna Arumugam, John R. Walker, Sadaf Valeh Sheida, Anja-Katrin Bielinsky, Markus C. Wahl, Jean-Yves Masson, and Xu-Dong Zhu

SUPPLEMENTAL Information

Document S1: Supplemental FIGURES S1-S10, Supplemental Table S1,

and Data S1/Methods S1

Supplemental Figure S1

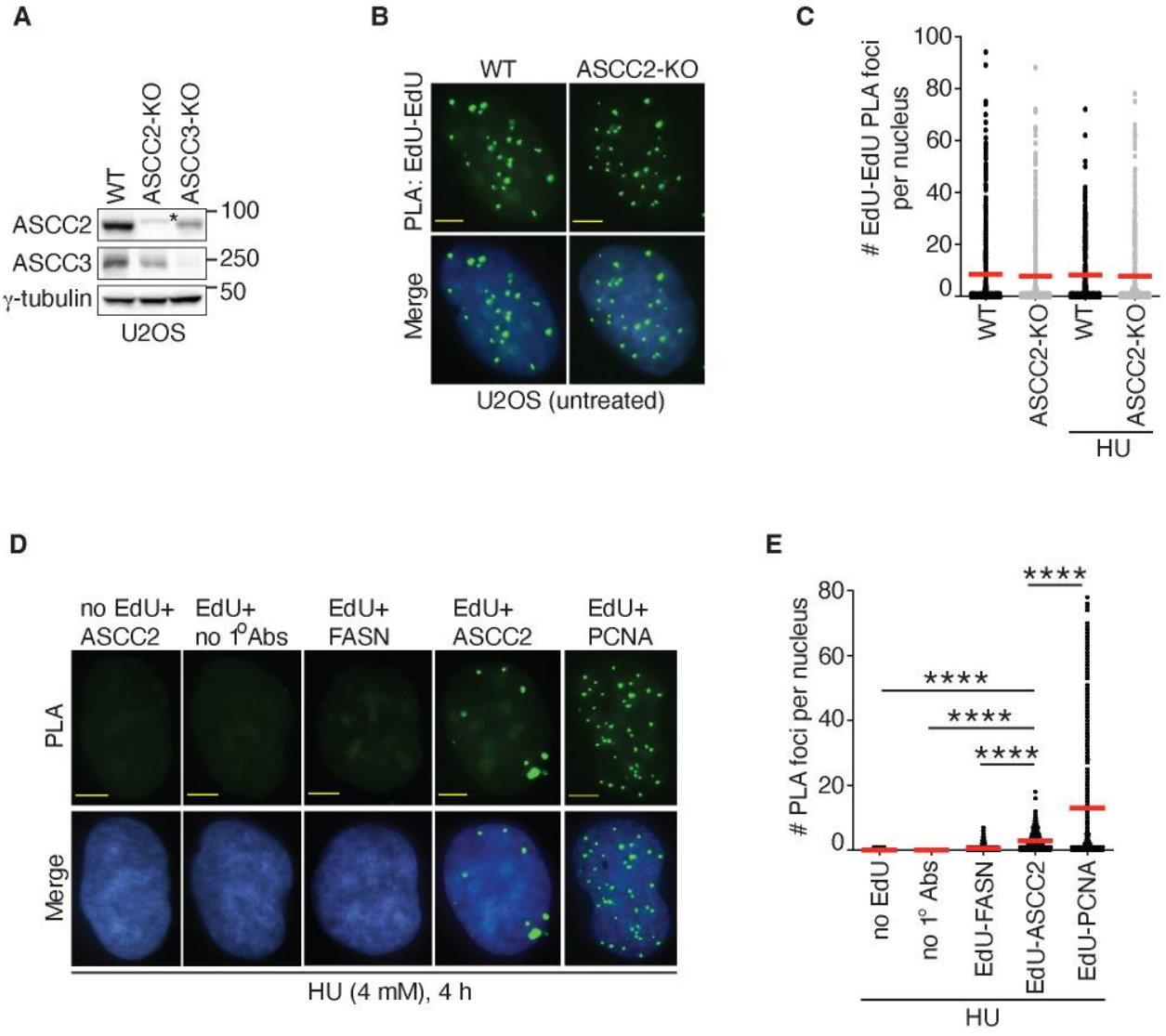

Figure S1. Recruitment of ASCC2 to stalled forks is not due to non-specific effects. (**A**) Western blot analyses of U2OS WT, ASCC2-KO, and ASCC3-KO cells. Immunoblotting was performed with anti-ASCC2, anti-ASCC3, and anti-γ-tubulin antibodies. The γ-tubulin blot was used as a loading control in this and subsequent figures except for where the α-tubulin blot was used as a loading control. The asterisk (*) indicates a non-specific band. (**B**) Representative images of EdU-EdU PLA foci formation in U2OS WT and ASCC2-KO cells. Nuclei were stained with DAPI in blue in this and subsequent figures. Scale bars in this and subsequent figures: 5 μm. (**C**) Quantification of EdU-EdU PLA foci formation. This PLA experiment was performed twice independently with reproducible results. Data from one representative experiment are shown as scatter plot graphs with the mean indicated in this and subsequent panels. A total of 439 cells per condition were analyzed. (**D**) Representative images of PLA foci formation in U2OS cells treated with 4 mM HU for 4 h. PLA assays were performed in several conditions as indicated above the images. (**E**) Quantification of PLA foci formation from (D). This PLA experiment was performed once. A total of 492-515 cells per condition were analyzed. ****P<0.0001 by Mann-Whitney rank-sum t-test.

Supplemental Figure S2

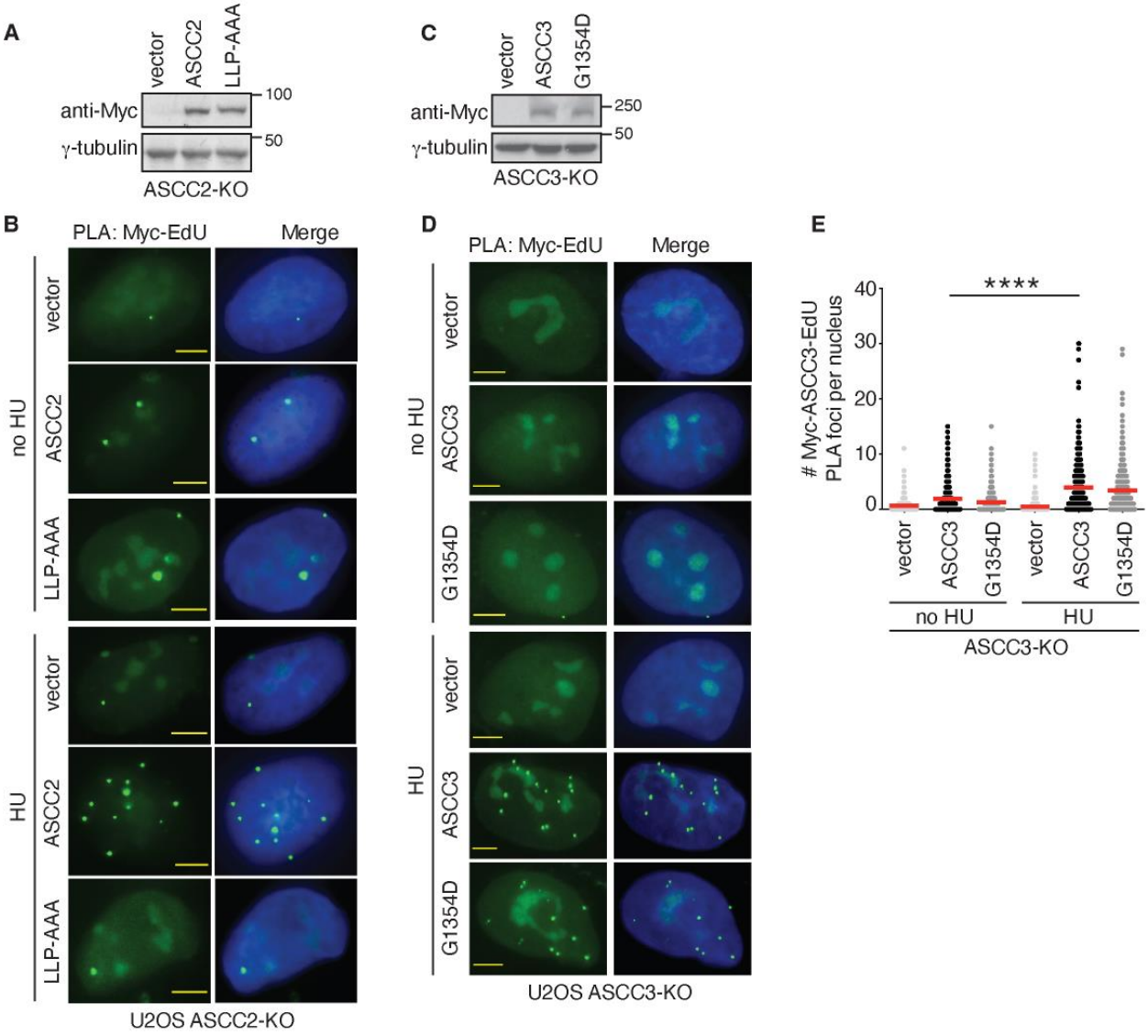

Figure S2. ASCC2 and ASCC3 are recruited to stalled forks, the former requiring its ubiquitin binding activity. (**A**) Western blot analyses of U2OS ASCC2-KO cells expressing various Myc-ASCC2 alleles as indicated. Immunoblotting was performed with anti-Myc and anti-γ-tubulin antibodies. (**B**) Representative images of Myc-EdU PLA foci formation in no HU- or HU-treated U2OS ASCC2-KO cells expressing various Myc-ASCC2 alleles as indicated. (**C**) Western blot analyses of U2OS ASCC3-KO cells expressing various Myc-ASCC3 alleles as indicated. Immunoblotting was performed with anti-Myc and anti-γ-tubulin antibodies. (**D**) Representative images of Myc-EdU PLA foci formation in no HU- or HU-treated U2OS ASCC3-KO cells expressing various Myc-ASCC3 alleles as indicated. (**E**) Quantification of Myc-ASCC3-EdU PLA foci formation in no HU- or HU-treated U2OS ASCC3-KO cells expressing various Myc-ASCC3 alleles as indicated. This PLA experiment was performed once. Data are represented as scatter plot graphs with the mean indicated. A total of 801-813 cells per condition were analyzed. ****P<0.0001 by Mann-Whitney rank-sum t-test.

Supplemental Figure S3

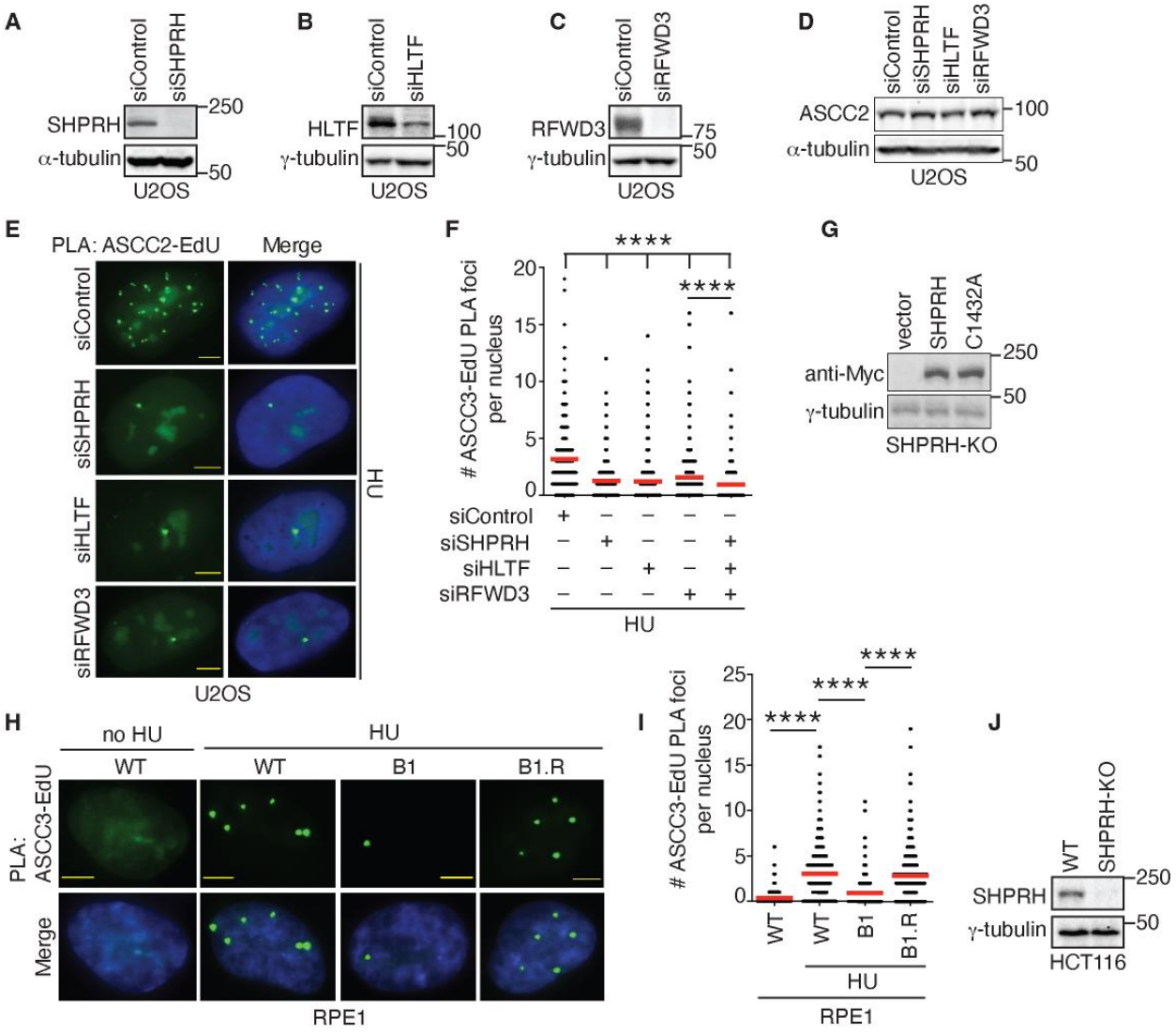

Figure S3. SHPRH, HLTF, and RFWD3 mediate recruitment of ASCC2 and ASCC3 to stalled forks. (**A**) Western blot analyses of U2OS cells transfected with siControl or siSHPRH. (**B**) Western blot analyses of U2OS cells transfected with siControl or siHLTF. (**C**) Western blot analyses of U2OS cells transfected with siControl or siRFWD3. (**D**) Western blot analyses of U2OS cells transfected with indicated siRNAs. Immunoblotting was performed with anti-ASCC2 and anti-α-tubulin antibodies. (**E**) Representative images of ASCC2-EdU PLA foci formation in HU-treated U2OS transfected with indicated siRNAs. (**F**) Quantification of ASCC3-EdU PLA foci formation in HU-treated U2OS cells transfected with indicated siRNAs. The PLA experiments were performed once in this and S3I panels. Data are shown as scatter plot graphs with the mean indicated in this and S3I panels. A total of 407-426 cells per condition were analyzed. ****P<0.0001 by Mann-Whitney rank-sum t-test (S3F and S3I). (**G**) Western blot analyses of U2OS SHPRH-KO cells expressing various Myc-SHPRH alleles as indicated. Immunoblotting was performed with anti-Myc and anti-γ-tubulin antibodies. (**H**) Representative images of ASCC3-EdU PLA foci in RPE1 parental (WT), B1 (PCNA-K164R), and B1 revertant (B1.R, PCNA-K164) cells that were treated with or without HU. (**I**) Quantification of ASCC3-EdU PLA foci formation from (H). A total of 454-470 cells per condition were analyzed. ****P<0.001. (**J**) Western blot analyses of HCT116 WT and SHPRH-KO cells. Immunoblotting was performed with anti-SHPRH and anti-γ-tubulin antibodies.

Supplemental Figure S4

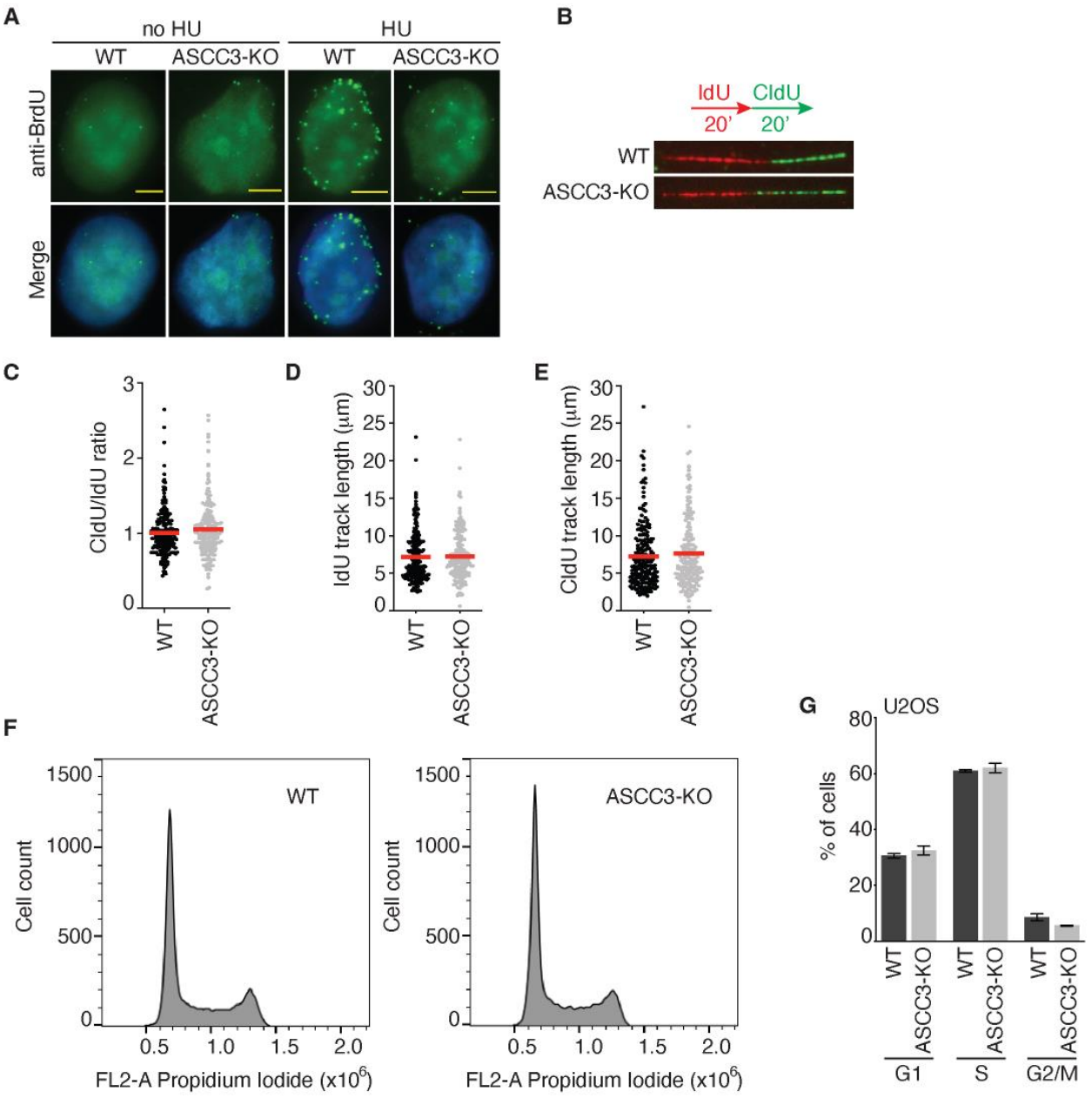

Figure S4. ASCC3 unwinds DNA upon replication stress. (**A**) Representative images of native BrdU staining in U2OS WT and ASCC3-KO cells that were pulse-labeled with BrdU prior to treatment with or without HU. (**B**) Representative images of DNA fibers from U2OS WT or ASCC3-KO cells that were first labeled with IdU and then CldU. (**C-E**) Quantification of the CldU/IdU ratios (C), the IdU track lengths (D), and the CldU track lengths (E) in U2OS WT and ASCC3-KO cells. This DNA fiber experiment was performed once. Data are represented as scatter plot graphs with the mean indicated. A total of 200-209 fibers per condition were analyzed. (**F**) Representative cell cycle profiles of U2OS WT and ASCC3-KO cells. (**G**) Quantification of the percentage of U2OS WT and ASCC3-KO cells in G1, S, and G2/M phases. SDs from three independent experiments are indicated.

Supplemental Figure S5

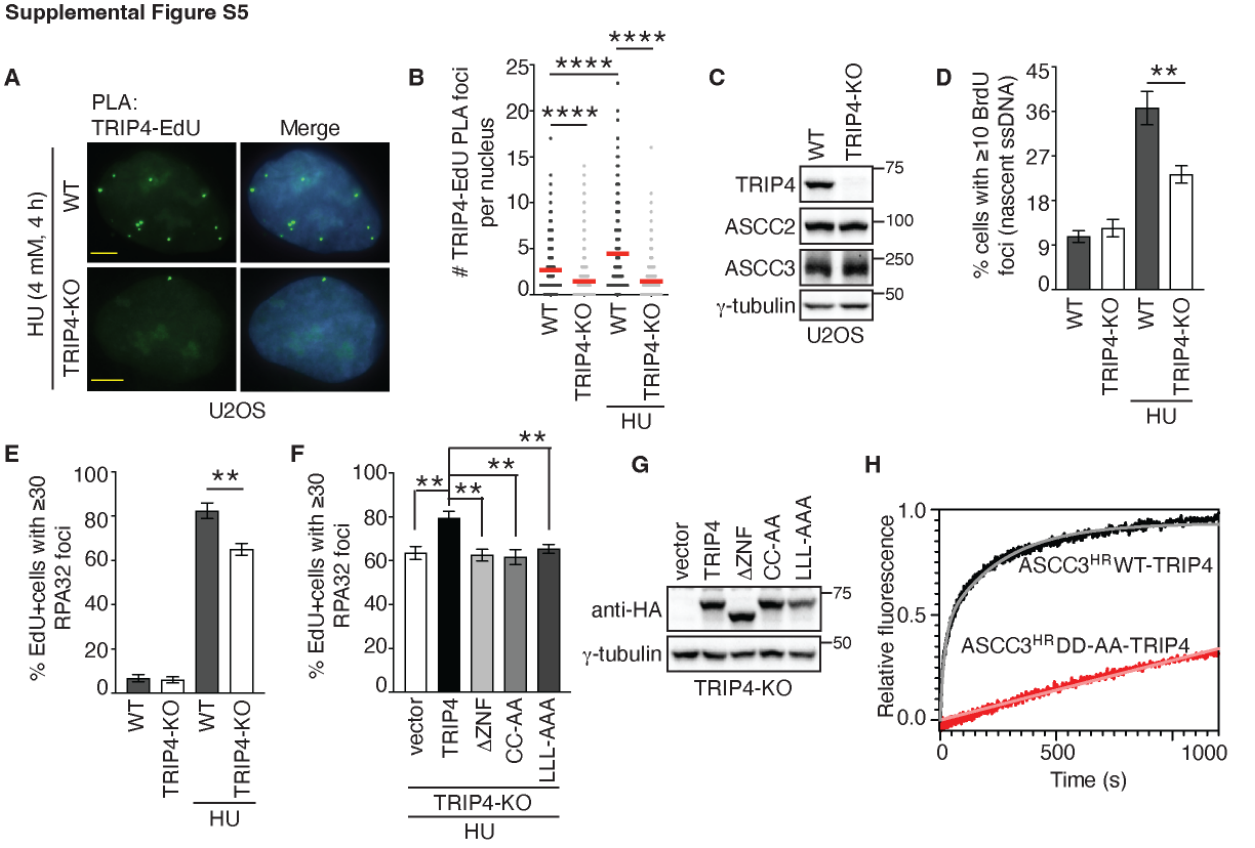

Figure S5. ASCC3 requires TRIP4 to promote RPA accumulation on ssDNA upon replication stress. (**A**) Representative images of endogenous TRIP4-EdU PLA foci formation in U2OS WT and TRIP4-KO cells treated with 4 mM HU for 4 h. (**B**) Quantification of endogenous TRIP4-EdU PLA foci formation from (A). The PLA experiments were performed once. Data are shown as scatter plot graphs with the mean indicated. A total of 420-433 cells per condition were analyzed. ****P<0.0001 by Mann-Whitney rank-sum t-test. (**C**) Western blot analyses of U2OS WT and TRIP4-KO cells. Immunoblotting was performed with anti-TRIP4, anti-ASCC2, anti-ASCC3, and anti-γ-tubulin antibodies. (**D**) Quantification of the percentage of cells with ≥ 10 BrdU foci. U2OS WT and TRIP4-KO cells were pulse-labeled with BrdU for 20 min and then treated with no HU or HU prior to fixation. A total of 601-650 cells per condition were scored in blind. SDs from three independent experiments are shown in this, S5E, and S5F panels. **P<0.01 by Student's t-test (S5D-S5F). (**E**) Quantification of the percentage of EdU+ cells with ≥ 30 RPA32 foci. U2OS WT and TRIP4-KO Cells were pulse-labeled with EdU for 10 min and then treated with or without HU prior to fixation in this and S5F panels. A total of 742-977 cells per condition were scored in blind. **P<0.01. (**F**) Quantification of the percentage of EdU+ cells with ≥ 30 RPA32 foci. U2OS TRIP4-KO cells were transfected with various HA-TRIP4 alleles as indicated. A total of 898-989 cells per condition were scored in blind. **P<0.01. (**G**) Western blot analysis of U2OS TRIP4-KO cells transfected with various HA-TRIP4 alleles as indicated. Immunoblotting was performed with anti-HA and anti-γ-tubulin antibodies. (**H**) In vitro helicase assays of ASCC3^{HR} WT-TRIP4 or ASCC3^{HR}-DD-AA-TRIP4 as indicated.

Supplemental Figure S6

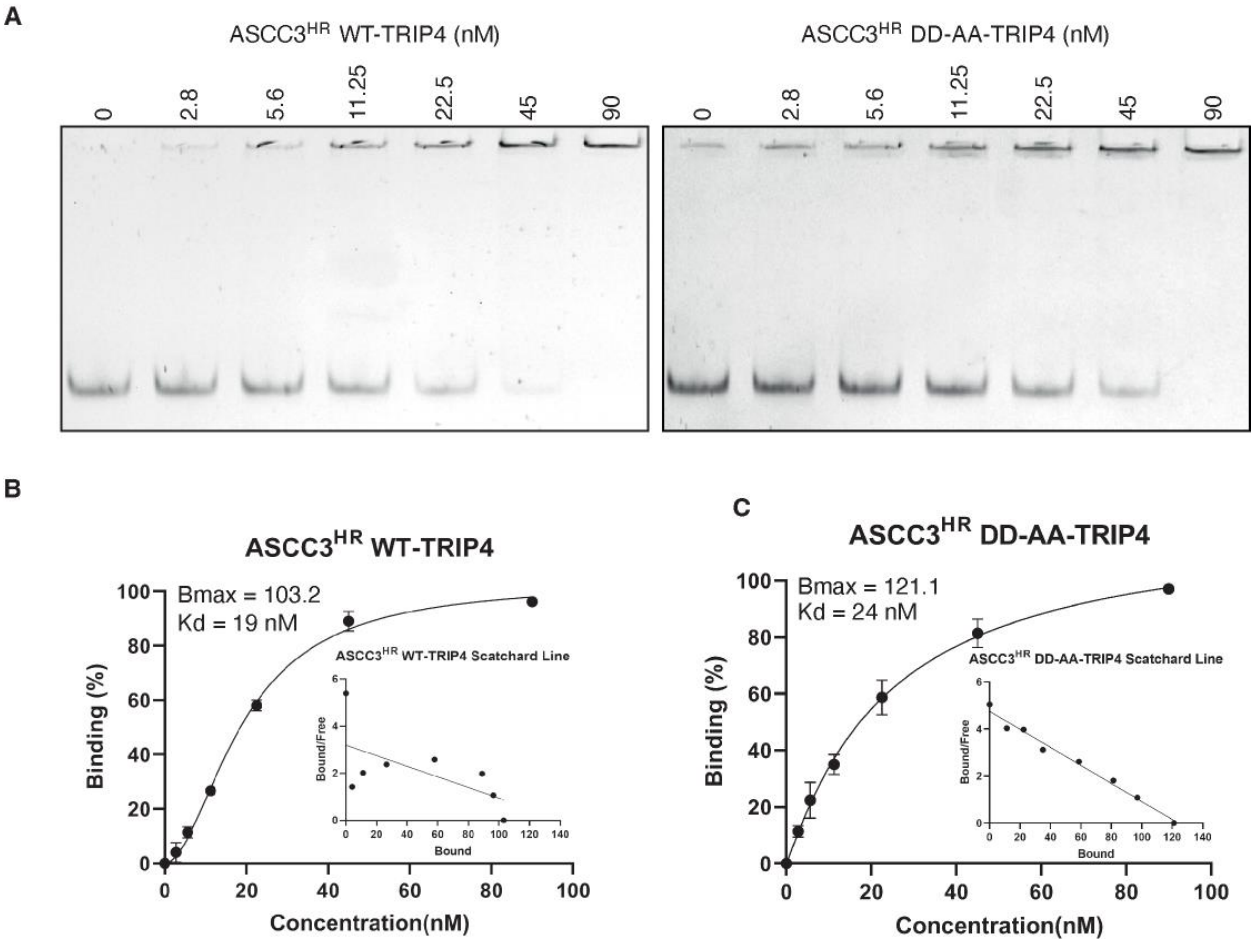

Figure S6. ASCC3 binds to dsDNA with a 3' overhang independently of its helicase activity. (**A**) Representative gel mobility shift assays by ASCC3^{HR} (WT or DD-AA)-TRIP4 on a 3'-tailed substrate. (**B and C**) Calculation of Kd and Bmax values for ASCC3HR WT-TRIP4 (B) and ASCC3HR-DD-AA-TRIP4 (C) using non-linear regression, based on the mean ± S.E.M. of three independent experiments.

Supplemental Figure S7

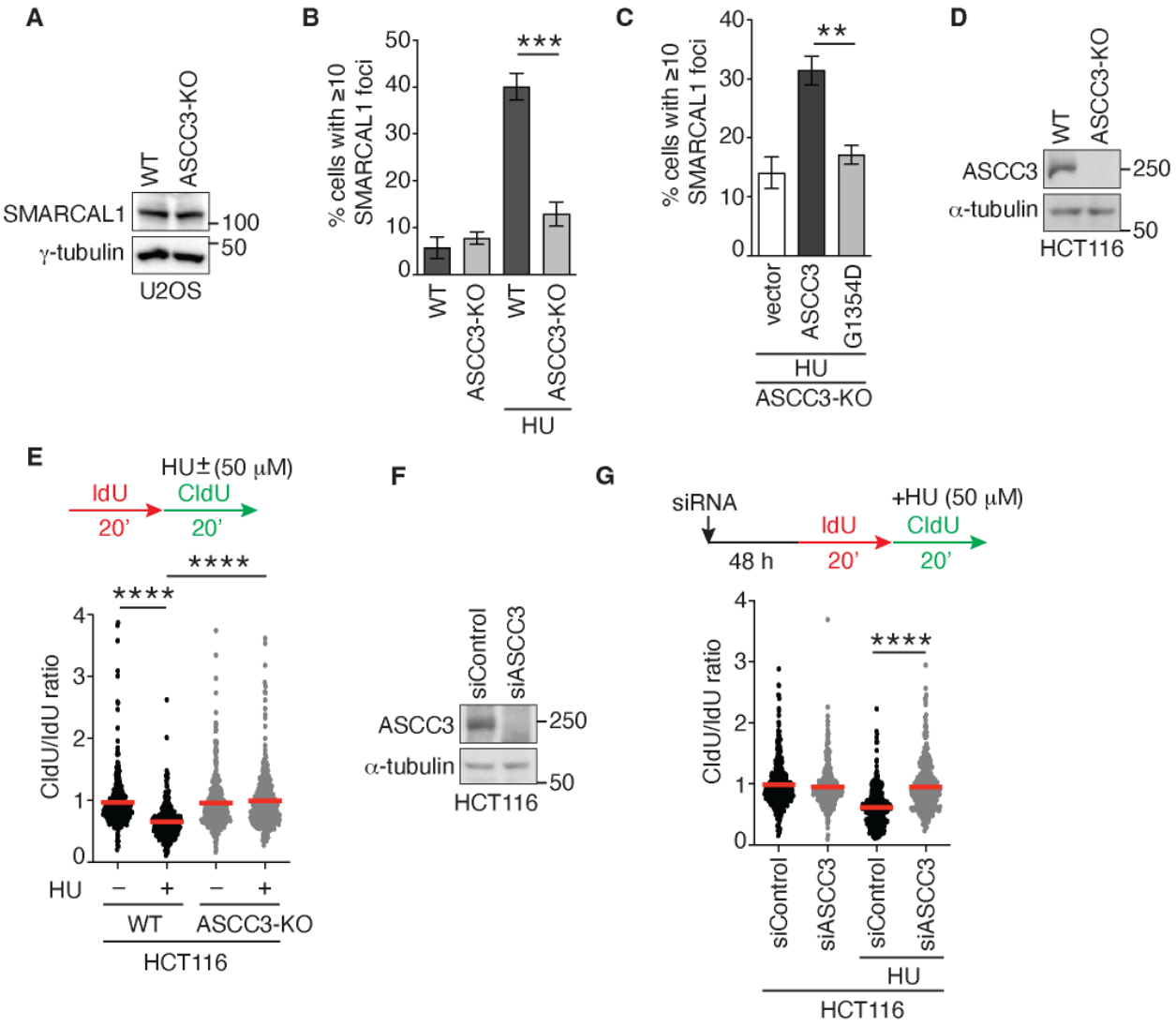

Figure S7. ASCC3 promotes SMARCAL1 recruitment and restrains fork progression upon replication stress. (**A**) Western blot analyses of U2OS WT and ASCC3-KO cells. (**B**) Quantification of the percentage of U2OS WT and ASCC3-KO cells with ≥ 10 SMARCAL1 foci. Cells were treated with or without 4 mM HU for 2 h prior to fixation. A total of 501-531 cells per condition were scored in blind. SDs from three independent experiments are indicated in this and S7C panels. ***P<0.001 by Student's t-test (S7B and S7C). (**C**) Quantification of the percentage of cells with ≥ 10 SMARCAL1 foci. U2OS ASCC3-KO cells were transfected with the vector alone, Myc-ASCC3, or Myc-ASCC3-G1354D prior to treatment with HU. A total of 501-537 cells per condition were scored in blind. **P<0.01. (**D**) Western blot analyses of HCT116 WT and ASCC3-KO cells. (**E**) Quantification of the CldU/IdU ratios in HCT116 WT and ASCC3-KO cells treated with or without HU. The DNA fiber experiments were performed twice independently with reproducible results in this and S7G panels. Data from one representative experiment are shown as scatter plot graphs with the mean indicated in this and S7G panels. A total of 308-317 fibers per condition were analyzed. ****P<0.0001 by Mann-Whitney rank-sum t-test (S7E and S7G). (**F**) Western blot analyses of HCT116 transfected with siControl or siASCC3. (**G**) Quantification of the CldU/IdU ratios in HCT116 cells that were transfected with siControl or siASCC3 prior to treatment with or without HU. A total of 407-413 fibers per condition were analyzed. ****P<0.0001.

Supplemental Figure S8

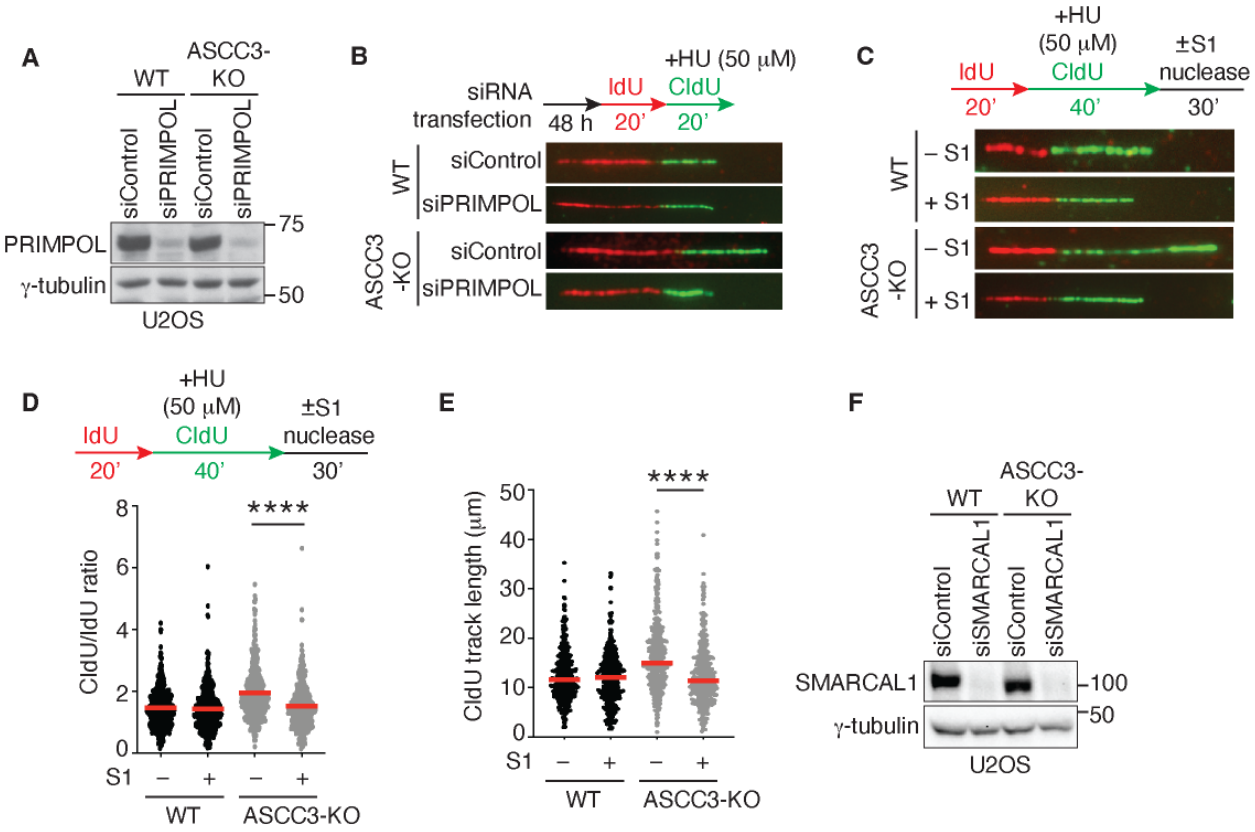

Figure S8. ASCC3 inhibits PRIMPOL-mediated fork repriming to restrain fork progression upon replication stress. (**A**) Western blot analyses of U2OS WT and ASCC3-KO cells transfected with control siRNA or siRNA against PRIMPOL (siPRIMPOL). Immunoblotting was performed with anti-PRIMPOL and anti-γ-tubulin antibodies. (**B**) Representative images of DNA fibers from HU-treated U2OS WT or ASCC3-KO cells that were transfected with control siRNA or siRNA against PRIMPOL. (**C**) Representative images of DNA fibers from HU-treated U2OS WT or ASCC3-KO cells that were treated with or without S1 nuclease. (**D and E**) Quantification of the CldU/IdU ratios (D) or the CldU track lengths (E) in U2OS WT and ASCC3-KO cells. Following HU treatment, these cells were treated with or without S1 nuclease. The DNA fiber assays were performed twice independently with reproducible results. Data from one representative experiment are shown as scatter plot graphs with the mean indicated. A total of 410-414 fibers per condition were analyzed. ****P<0.0001 by Mann-Whitney rank-sum t-test. (**F**) Western blot analyses of U2OS WT and ASCC3-KO cells transfected with indicated siRNAs. Immunoblotting was done with anti-SMARCAL1 and anti-γ-tubulin antibodies.

Supplemental Figure S9

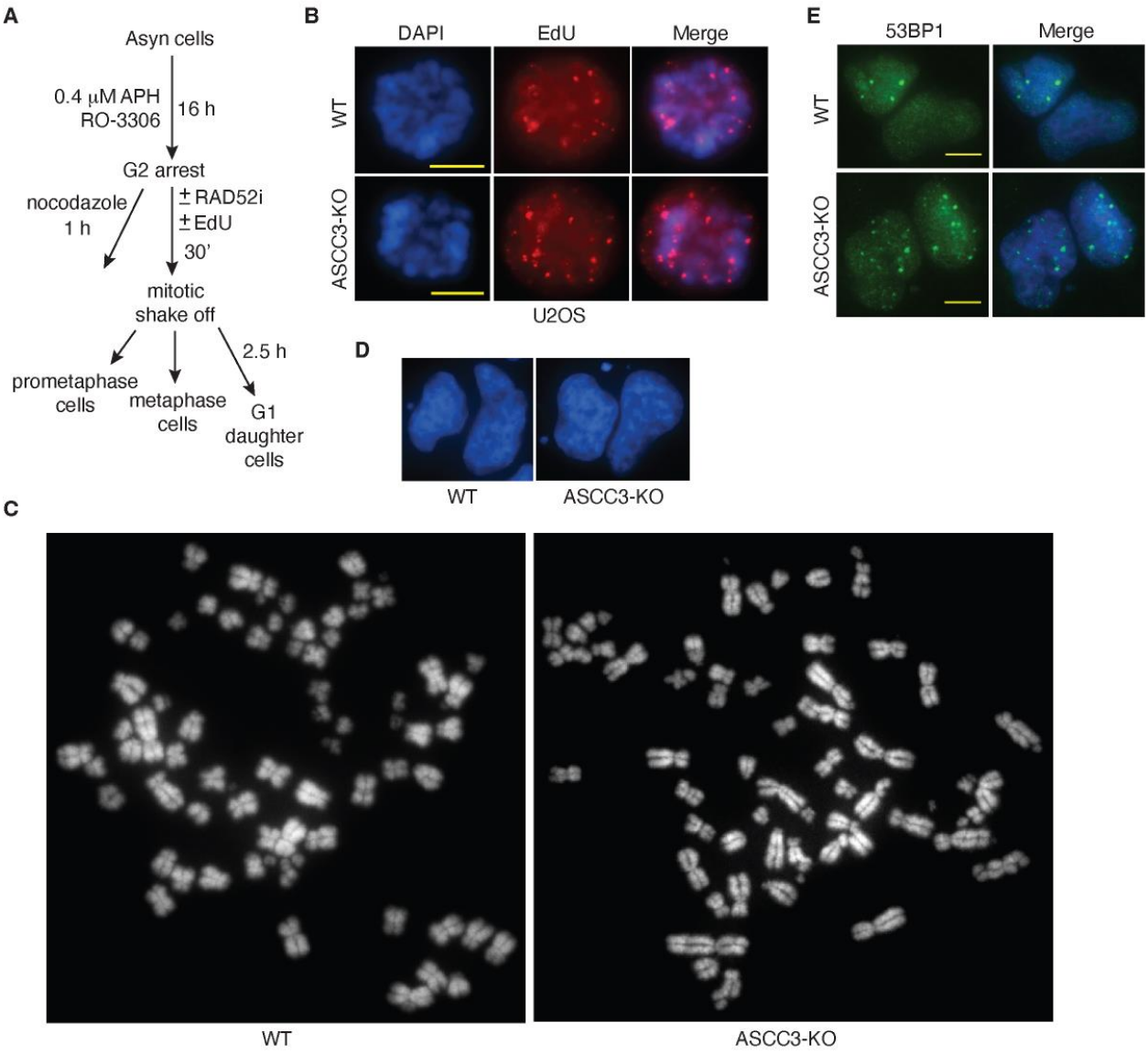

Figure S9. ASCC3 promotes genomic stability. (**A**) Schematic diagram of experimental setup. APH: aphidicolin; RO-3306: CDK1 inhibitor; RAD52i: RAD52 inhibitor AICAR. (**B**) Representative images of EdU foci in U2OS WT and ASCC3-KO prometaphase cells following exposure to 0.4 μM aphidicolin in S phase. (**C**) Representative images of metaphase chromosomes of U2OS WT and ASCC3-KO cells following exposure to 0.4 μM aphidicolin in S phase. (**D**) Representative images of micronuclei formation in U2OS WT and ASCC3-KO G1 daughter cells following exposure to 0.4 μM aphidicolin in S phase. (**E**) Representative images of the formation of 53BP1 nuclear bodies in U2OS WT and ASCC3-KO G1 daughter cells following exposure to 0.4 μM aphidicolin in S phase.

Supplemental Figure S10

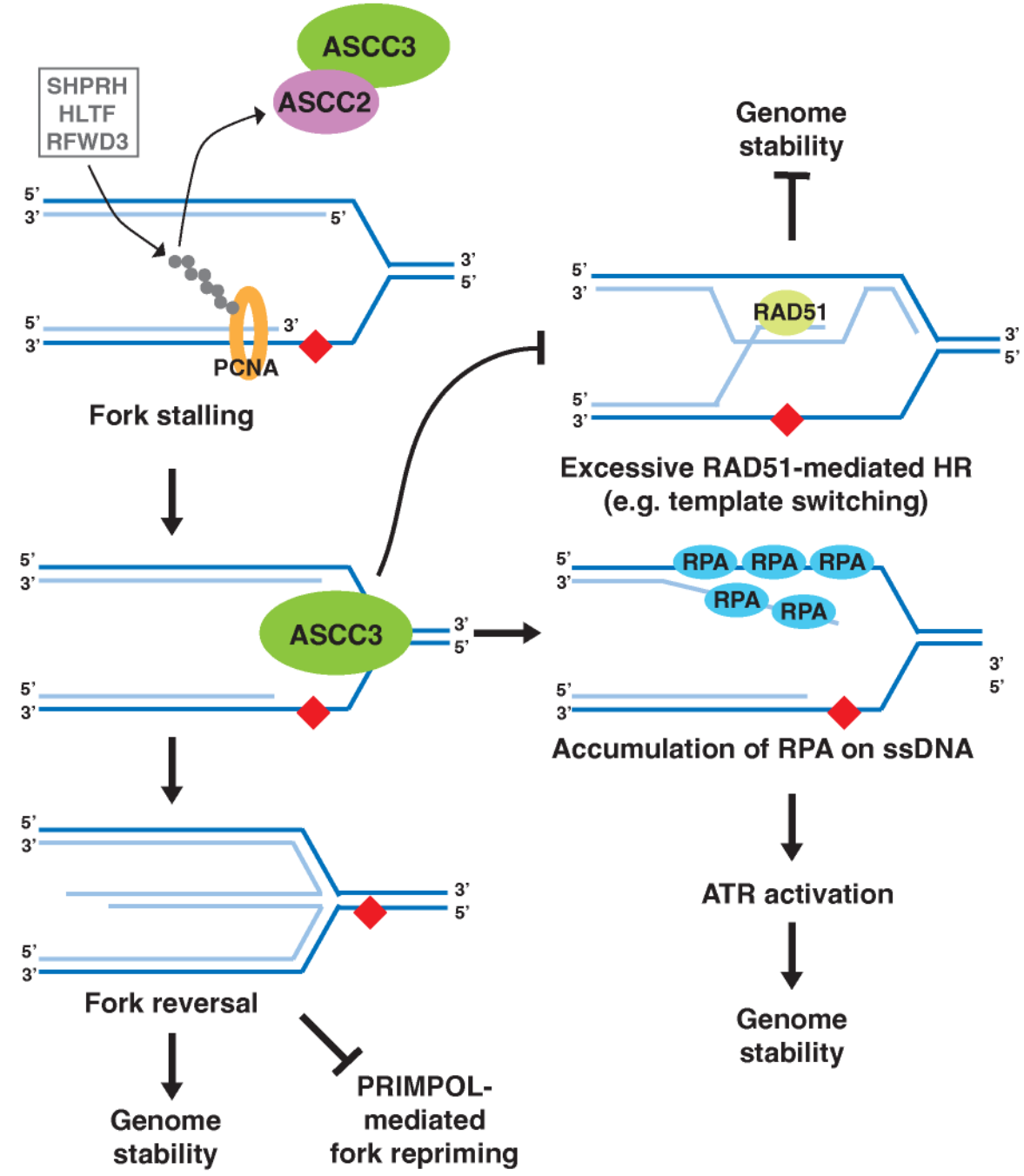

Figure S10. Model for the role of ASCC3 in controlling replication stress responses. We propose that ASCC2 binds PCNA polyubiquitylated at K164, which is catalyzed by SHPRH, HLTF, and RFWD3, and simultaneously recruits ASCC3 to stalled forks. In response to replication stress, ASCC3 unwinds DNA (likely with a preference for lagging strands since it requires the presence of 3' ssDNA). This unwinding activity is required for RPA accumulation on ssDNA, which promotes efficient ATR activation, as well as fork reversal. In addition, ASCC3 antagonizes RAD51-dependent HR activity, e.g. template switching, upon replication stress. Thus, ASCC3 controls multiple replication stress responses to maintain genomic stability.

Supplemental Table S1

siRNA	**Sequence (5' to 3')**
ASCC2	GGUAUUUUGUGUUAUACAA
ASCC3	GCAAGAUAAUUAUAAUGAA
CSB	GAAGAGUUGUCAGUGAUUA
HLTF	GGAAUAUAAUGUUAACGAU
PRIMPOL	GAGGAAAGCUGGACAUCGA
RAD51	AAGGGAAUUAGUGAAGCCAAA
RAD51	GAAGCUAUGUUCGCCAUUA
RFWD3	GGACCUACUUGCAAACUAU
SHPRH	GCACAAAUCAGUCGUGUUA
SMARCAL1	GAAUCUCACUUCCUCAAAA
TRIP4	CUUCAAAAAAGAUGAAAUU
USP1	GAAAUACACAGCCAAGUAA
Oligonucleotides	**Sequence**
Oligos used to generate DNA substrates for in vitro unwinding assays (complementary regions in bold)	Short strand 5'-**CGGCTCGCGGCC**-3'[Alexa488]
	Complementary strand [BHQ-1]5'- **GGCCGCGAGCCG**GAAATTTAATTATAAACCAGACCGTCTCCTC-3'
Oligos used in vitro assays (RPA binding and strand exchange)	100mer 5'- GGGCGAATTGGGCCCGACGTCGCATGCTCCTCTAGACTCGAGGAATTC GGTACCCCGGGTTCGAAATCGATAAGCTTACAGTCTCCATTTAAAGGA CAAG-3'
	75mer 5'- GCTTATCGATTTCGAACCCGGGGTACCGAATTCCTCGAGTCTAGAGGA GCATGCGACGTCGGGCCCAATTCGCCC-3'
	27mer 3'-CCCGCTTAACCCGGGCTGCAGCGTACG-5'
	35mer 5'-AGGAATTCGGTACCCCGGGTTCGAAATCGATAAGC-3'
Oligos used in DNA binding and fork reversal assays	JYM1413 5'- GGGCGAATTGGGCCCGACGTCGCATGCTCCTCTAGACTCGAGGAATTC GGTACCCCGGGTTCGAAATCGATAAGCTTACAGTCTCCATTTAAAGGA CAAG-3'[665 nm fluorophore]
	JYM6231 5'- GCTTATCGATTTCGAACCCGGGGTACCGAATTCCTCGAGTCTAGAGGA GCATGCGACGTCGGGCCCAATTCGCCC-3'
	JYM6376

	[665 nm fluorophore]5’- AGCTACCATGCCTGCCTCAAGAATTCGTAATATGCCTACACTGGAGTAC CGGAGCATCGTCGTGACTGGGAAAAC-3’
	JYM5395 5’-TTACGAATTCTTGAGGCAGGCATGGTAGCT-3’
	JYM6377 [665 nm fluorophore]5’-AGCTACCATGCCTGCCTCAAGAATTCGTAA-3’
	JYM5397 5’- GTTTTCCCAGTCACGACGATGCTCCGGTACTCCAGTGTAGGCATATTAC GAATTCTTGAGGCAGGCATGGTAGCT-3’
	JYM6375 5’-TTGAGGCAGGCATGGTAGCT-3’

Data S1/Methods S1: Raw images for Figures 3K, 5A, 5G, and 6F

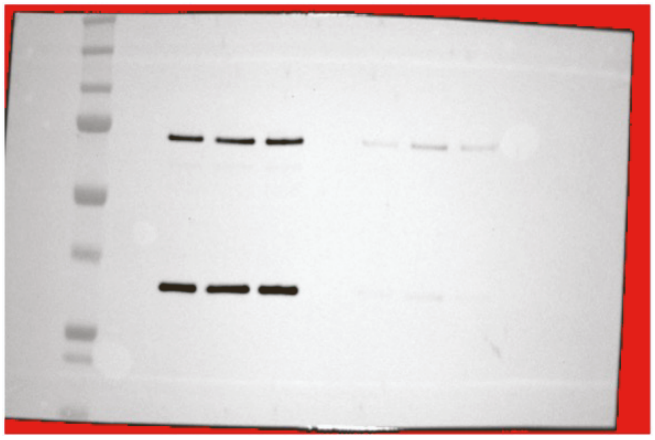

Raw image for Figure 3K

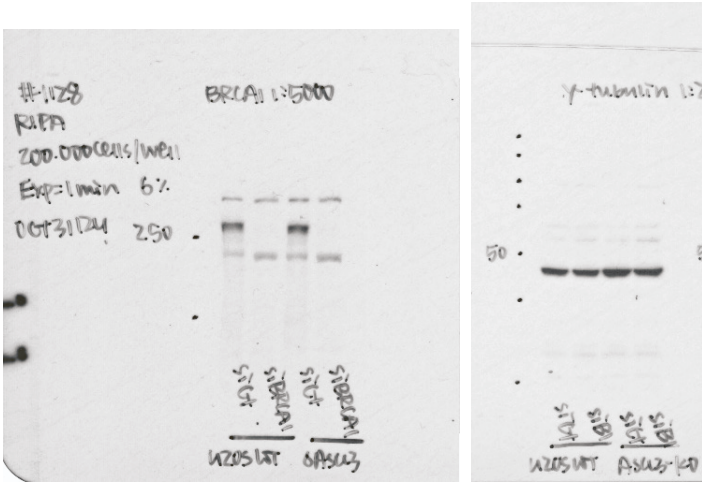

Raw images for Figure 5A

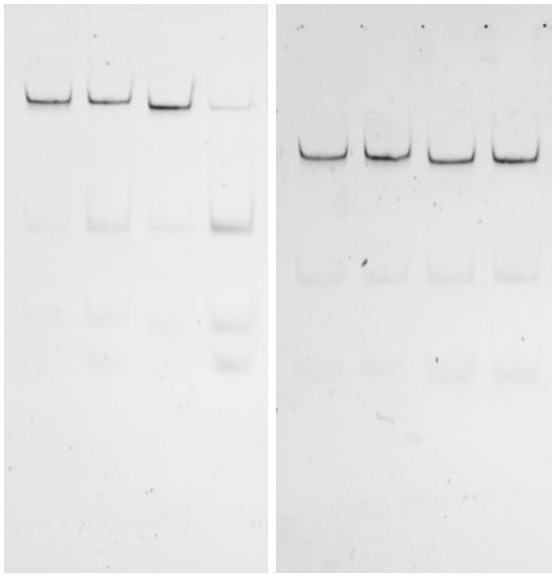

Raw images for Figure 5G

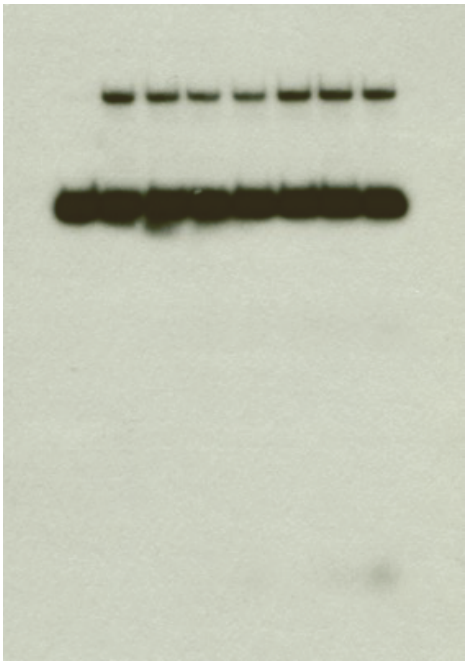

Raw image for Figure 6F